Trypsin immobilization in ordered porous polymer membranes for effective protein digestion

Juan Qiao [a,1], Jin Yong Kim [b,1], Yuan Yuan Wang [a], Li Qi [a,*], Fu Yi Wang [a], Myeong Hee Moon [b,**]

[a] Beijing National Laboratory for Molecular Sciences; Key Laboratory of Analytical Chemistry for Living Biosystems, Institute of Chemistry, Chinese Academy of Sciences, No. 2 Zhongguancun Beiyijie, Beijing 100190, PR China
[b] Department of Chemistry, Yonsei University, 50 Yonsei-ro, Seoul 120-749, South Korea

HIGHLIGHTS

- A porous polymer membrane enzyme reactor was developed.
- Breath figure method was used for the fabrication of porous polymer membrane.
- The enzyme reactor was coupled to nLC-ESI-MS/MS for proteins on-line digestion.

GRAPHICAL ABSTRACT
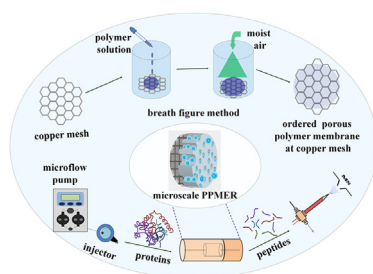
ARTICLE INFO

ABSTRACT

Fast and effective protein digestion is a vital process for mass spectrometry (MS) based protein analysis. This study introduces a porous polymer membrane enzyme reactor (PPMER) coupled to nanoflow liquid chromatography-tandem MS (nLC-ESI-MS/MS) for on-line digestion and analysis of proteins. Poly (styrene-co-maleic anhydride) (PS-co-MAn) was fabricated by the breath figure method to make a porous polymer membrane in which the MAn group was covalently bound to enzyme. Based on this strategy, microscale PPMER (μPPMER) was constructed for on-line connection with the nLC-ESI-MS/MS system. Its capability for enzymatic digestion with bovine serum albumin (BSA) was evaluated with varied digestion periods. The on-line proteolysis of BSA and subsequent analysis with μPPMER-nLC-ESI-MS/MS revealed that peptide sequence coverage increased from 10.3% (digestion time 10 min) to 89.1% (digestion time 30 min). μPPMER can efficiently digest proteins due to the microscopic confinement effect, showing its potential application in fast protein identification and protease immobilization. Applications of on-line digestion using μPPMER with human plasma and urinary proteome samples showed that the developed on-line method yielded equivalent or better performance in protein coverage and identified more

membrane proteins than the in-solution method. This may be due to easy accommodation of hydrophobic membrane proteins within membrane pores.

1. Introduction

Proteolysis is a vital and well-established preliminary step in mass spectrometry (MS) based protein analysis [1,2]. The typical in-solution digestion method utilizes low concentration proteases to avoid sample contamination and self-digestion of the enzyme. In-solution proteolysis is generally slow and inefficient at digesting proteins that are in low concentrations. To resolve this problem, enzyme immobilization methods have been widely developed with on-line enzymatic reactors. These methods are based on protease immobilization on solid substrates such as microchips [3—5], membranes [6,7], nanoparticles [8—15], porous glasses [16,17], and monolith [18,19] or on entrapment of enzymes within hollow fibers for proteolysis or deglycosylation [20,21].

Nanoporous materials, including carbon nanotubes [22,23], and mesoporous silica [24—26], have attracted interest for their biological applicability. Advantages of these materials include their large specific surface area and tunable pore size. These pores can accommodate proteases from small globular proteins with diameters of a few nanometers to large enzyme molecules [27]. The method increases the reaction efficiency of enzymes immobilized by porous materials. The enhanced efficiency originates from local increases in the concentration of immobilized enzymes compared to that of in-solution digestion processes. The time-consuming protein-enzyme processes of in-solution digestion are replaced with a rapid process of protein entrapment in nanopores followed by proteolysis.

Since porous materials enhance digestion efficiency, a number of porous materials have been explored. Proteases immobilized on nanoporous membranes can digest protein in a few minutes and lead to high peptide coverage compared to the in-solution method. Several kinds of porous membranes have been utilized for enzyme immobilization, including nylon membranes [28—30]. Electrostatic interactions between enzyme and membranes were commonly utilized for enzyme immobilization. While the inner surface of nanopores can be used for electrostatic adsorption of enzyme, this approach is relatively inefficient due to continuous bleeding of enzymes [31]. Covalent linkage is a suitable alternative used to immobilize proteases at the surface of nanoporous membranes and avoid bleeding enzyme molecules. Membranes with ordered nanopores containing multifunctional groups for covalent enzyme immobilization are excellent candidates.

The recently developed breath figure method exhibits a few advantages, such as simple preparation of ordered polymeric porous membranes using polymers dissolved in volatile organic solvent exposed to moisturized air flow [32,33]. A variety of polymers [32] have been employed in the formation of ordered microporous films with pore diameters ranging from 100 nm to 20 μm, including comb-like copolymers, star polymers, linear homopolymers, hyperbranched polymers, and rod-coil/coil—coil block copolymers. Importantly, these porous polymers possess multifunctional groups that readily react with enzymes. To the best of our knowledge, porous polymer membrane enzyme reactors fabricated by the breath figure method are not frequently reported because they are fragile, with poor durability and tenacity.

This study introduces a novel strategy for overcoming the shortcomings of microporous membrane based enzyme reactors fabricated by the breath figure method. First, a block copolymer made of poly styrene-*co*-maleic anhydride (PS-*co*-MAn) was utilized to construct polymer membranes with MAn groups that easily react with enzyme (i.e. trypsin) in moderate conditions. The breath figure method was effective for fabricating ordered porous polymer membranes due to the presence of both hydrophilic and hydrophobic segments in the PS-*co*-MAn framework. Copper mesh was utilized as a solid substrate of the membrane enzyme reactors to overcome the weakness of poorly tenacious membranes and increase their durability for repeated usage. The PS-*co*-MAn based porous polymer membrane enzyme reactor (PPMER) developed in this study was integrated as a microscale reactor prior to nanoflow liquid chromatography-tandem mass spectrometry (nLC-ESI-MS/MS) for on-line high speed protein digestion and proteomic analysis. The performance of microscale PPMER (μPPMER) for proteolysis was evaluated with bovine serum albumin (BSA) and cytochrome C (Cyt C) by examining protein sequence coverage, minimum amount of protein handled, and reproducibility with nLC-ESI-MS/MS. Finally, the developed on-line method was applied to pooled human plasma to compare its performance with that of the in-solution digestion method. The present study demonstrates great potential for μPPMER applications in rapid and effective proteolysis of a small amount of proteins.

2. Experimental

2.1. Chemicals and materials

Styrene (St) and MAn monomers were obtained from Sinopharm Chemical Reagent Beijing Co., Ltd (Beijing, China) and Tianjin Guangfu Fine Chemical Research Institute (Tianjin, China), respectively. The chain transfer reagent for reversible addition—-fragmentation chain transfer (RAFT) polymerization, S,S'-bis (α, α'-dimethylacetic acid) trithiocarbonate (DATB), was synthesized according to the reference [34]. The RAFT polymerization initiator, azo-bis-isobutryonitrile (AIBN), was obtained from Shanghai Chemical Plant (Shanghai, China). N-*a*-benzoyl-ʟ-arginine ethyl ester (BAEE) was obtained from Acros Organics (Fair Lawn, NJ, USA). N-*a*-Benzoyl-ʟ-arginine (BA) was purchased from Aladdin Reagents Industrial Co., Ltd (Shanghai, China). Analytical reagent grade organic solvents, including 1,4-dioxane and ether, were obtained from Beijing Chemical Factory (Beijing, China). Trypsin, cytochrome C, and BSA were purchased from Sigma (St. Louis, MO, USA). Copper mesh (50 μm in thickness) was obtained from Huawei hardware store (Beijing, China). Water used throughout the experiments was purified by a Milli-Q water purification system (Millipore, Bedford, MA, USA). Human plasma and urine samples were obtained from 3 healthy adults of Severance Medical Center (Seoul, Korea), and each group was pooled together.

2.2. Apparatus

A model S-4800 scanning electron microscope (SEM) from Hitachi Co. (Hitachi, Japan) was used to examine the morphology of copper mesh and ordered porous membrane made by the breath figure method.

The molecular weight and polydispersity index (PDI) of PS-*co*-

MAn were determined by gel permeation chromatography (GPC) equipped with a model L-2130 HPLC pump from Hitachi Co., a model 2410 refractive index detector and a model 2487 ultraviolet detector both from Waters Co. (Milford, MA, USA), using a combination of MZ-Gel SDplus columns (5 μm, porosity of 10^3, 10^4, and 10^5 Å) from MZ-Analysentechnik GmbH (Mainz, Germany). THF was used as the eluent at a flow rate of 1.0 mL/min, and polystyrene standards (MW of 1.3 K, 3.3 K, 5.2 K, 13.0 K and 25.0 K) were used for calibration.

The porosity and pore size distribution of membranes were measured by Autopore IV 9510 mercury porosimetry from Micromeritics Instrument Co. (Norcross, GA, USA).

2.3. Preparation of ordered porous polymer membranes

Fig. 1 represents the preparation of porous polymer membranes on copper mesh eroded with hydrochloric acid and heated at 500 °C for 2 h. The eroded copper mesh was used as a solid substrate and was placed in a humid (relative humidity 90%) environment prepared by a humidifier. The PS-co-MAn solution (30.0 mg mL^{-1}, dissolved in chloroform) was then cast onto the eroded copper mesh. After all solvent molecules were evaporated, ordered porous polymer membranes were formed on the substrate.

2.4. Fabrication of PPMER

Ordered porous polymer membranes on copper mesh (hereafter referred to as membrane unit) were cut and put into a permeation module (diameter 1.2 cm) from Beijing Xinjingke Biotechnology Co., Ltd (Beijing, China), which is often used for sample pretreatment. The inserted membrane unit was washed with 30 mL Tris-HCl buffer solution (0.10 M, pH 8.4). Then, 2.0 mg/mL trypsin in 0.10 M Tris-HCl and 50 mM benzamidine was circulated through the module at a flow rate of 10.0 μL/min for 24 h to prepare PPMER. The membrane unit inside PPMER was then cleaned with a PBS buffer rinse. The amount of enzyme immobilized onto porous polymer membrane was determined by a Bradford assay [35], as described in Supporting Information, and calculated from the difference in enzyme solution concentrations before and after circulating the enzyme solution through PPMER. The activity of immobilized trypsin was evaluated with BAEE (ranging from 0.1 mM to 8.0 mM) from the apparent kinetic parameters of Michaelis−Menten's constant (K_m) and maximum rate (V_{max}), as described in Supporting Information.

2.5. Reproducibility and stability of PPMER

The hydrolysis yields of substrate BAEE were applied in evaluation of the reproducibility and stability of immobilized enzyme.

The hydrolysis yields of substrate BAEE (5.0 mM) under different conditions were studied, including reusability after nine times and stability for four weeks.

2.6. Assembly of μPPMER module

The μPPMER module for on-line connection with nLC-ESI-MS/MS analysis was assembled by inserting the prepared porous polymer membrane unit with copper mesh into a PEEK Precolumn filter unit (1.4 μL of original swept volume) from IDEX Health & Science, LCC (Oak Harbor, WA, USA). This was followed by immobilizing trypsin onto the membrane unit, as illustrated in Figure S1 (Supporting Information). To provide extra space for enzyme above membrane, the membrane unit was placed underneath the PCFTE (polychlorotrifluoroethylene) ring (o.d. 0.25, i.d. 0.188, thickness 0.062 inch), which is the siding of the original PEEK frit unit. The calculated volume of μPPMER space was ~29 μL. The inlet and outlet of the on-line μPPMER module were connected with a fused silica capillary tube (o.d. 360 μm and i.d. 200 μm) from Polymicro Technology LCC (Phoenix, AZ, USA).

2.7. Enzyme immobilization of μPPMER module

At the surface of polymer coated copper mesh, enzymes were immobilized by injecting enzyme into the inner space of the microscale μPPMER module via a model 7725i loop injector (Rheodyne, Cotati, CA, USA) using 50 mM tris-buffered saline (TBS, pH 8.4) solution and a model Legato 110 syringe pump from KD Scientific (Holliston, MA, USA). For each immobilization procedure, 20 μg of sequential grade modified trypsin from Promega Corp. (Madison, WI, USA) was injected with a pump flow rate of 5 μL/min. For immobilization, the μPPMER unit was pumped for 12 h. During enzyme immobilization, an extra cellulose membrane with a molecular weight cut-off of 10 kDa from Merck Millipore (Billerica, MA, USA) was placed underneath the copper mesh, as shown in Figure S1a (Supporting Information). This kept enzyme from passing through the polymer coated copper mesh and ensured enzyme immobilization. Once enzyme immobilization was completed, the extra cellulose membrane was removed. To isolate or purify digested molecules, the enzyme immobilized μPPMER module was connected to a microflow pump from FLOM Corp. (Tokyo, Japan), shown in Figure S1b (Supporting Information), and to a trapping column (explained in the following section).

2.8. Preparation of human plasma and urine samples for on-line proteomic analysis

A protease inhibitor cocktail tablet from Hoffmann-La Roche Ltd (Basel, Switzerland) was added to 10 mL of raw urine sample
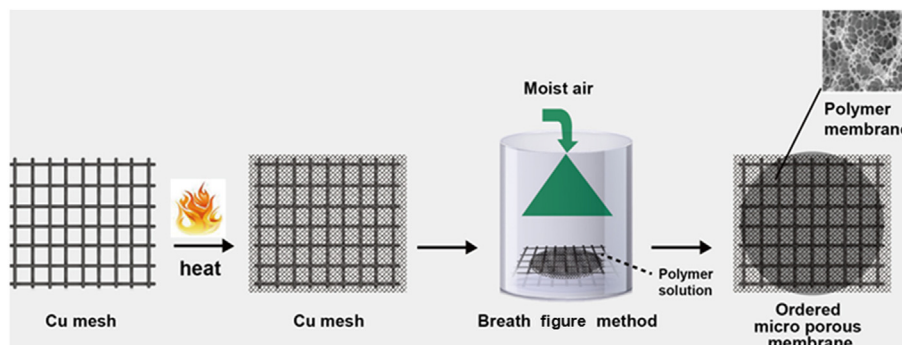

Fig. 1. Fabrication of porous polymer membrane.

(pooled) and then centrifuged at 300-g. The supernatant solution was removed to calculate concentration using Amicon Ultracel-3K centrifugal filter units from Millipore (Danvers, MA, USA). For the pooled plasma sample, albumin and IgG were first depleted using a ProteoPrep Immunoaffinity Albumin & IgG Depletion kit from Sigma Aldrich. The concentration of proteins in each prepared sample was determined as 2.18 and 3.08 mg/mL for urine and plasma, respectively, by a Bradford assay using Bradford reagent from Bio-Rad Laboratories, Inc. (Hercules, CA, USA).

2.9. On-line μPPMER-nLC-ESI-MS/MS analysis

On-line coupling of the μPPMER module with nLC-ESI-MS/MS was assembled by connecting μPPMER to a pulled-tip capillary LC column via a 6-port switching valve, as shown in Fig. 2. Prior to the LC column, a capillary trapping column (100 μm-i.d. × 360 μm-o.d.) ending with sol–gel frit which was packed with 3 μm-200 Å Magic C18AQ beads from Michrom Bioresources Inc. (Auburn, CA, USA) for 0.5 cm was used to capture digested peptides eluted from μPPMER. The analytical column (75 μm i.d. × 360 μm o.d. × 15 cm) was prepared in the laboratory by packing 3 μm-100 Å Magic C18AQ beads in a capillary tube with one end pulled into a sharp needle using flame for a direct ESI.

On-line proteolysis began by loading the protein sample to the μPPMER module at a flow rate of 5 μL/min of carrier solution and 10 mM phosphate buffered saline (PBS) with 10 mM dithiothreitol (DTT) for protein denaturation. A microflow pump was used, as shown in the solid line configuration of Fig. 2. Product peptides eluted from μPPMER were captured in the trapping column while non-retaining species were evacuated from the system through a microcross waste port, shown in Fig. 2. The enzymatic reaction time was optimized by varying reaction periods. Once proteolysis was completed, the 6-port valve was changed into the dotted line configuration (Fig. 2) to carry out nLC-ESI-MS/MS analysis. nLC-ESI-MS/MS was equipped with a model 1260 capillary LC system from Agilent Technologies (Waldbronn, Germany) interfaced with a LTQ Velos ion trap mass spectrometer from Thermo Finnigan (San Jose, CA, USA). The mobile phases for binary gradient elution were 98/2 (v/v) water/acetonitrile for A and 95/5 (v/v) acetonitrile/water for B. Both solutions were added with 0.1% formic acid for electrospray

ionization (ESI) of peptides. Before gradient elution began, 2% of mobile phase B was delivered to the trapping column for 10 min to remove remaining salts in the trapping column. The gradient step began with an initial increase to 10% B for 1 min. Mobile phase B was gradually increased to 50% for 53 min, ramped to 80% for 3 min, and then maintained at 80% for 10 min to allow column cleaning. It then returned to 2% for 3 min, and at least 20 min was allowed at 2% B for column re-conditioning. The flow rate of the column outlet for nLC-ESI-MS/MS was 200 nL/min.

For ESI, 2.5 kV was applied in positive ion mode. A MS precursor scan was carried out in the *m/z* range of 300–1800, and collision induced dissociation (CID) experiments were made using a data-dependent mode for the three prominent precursor ions. Proteome Discoverer software (Ver 1.2.0.208) from Thermo Finnigan, with false positive options based on the nrNCBI human database, was used to identify peptides (mass tolerance value: 1.0 Da for precursor ions and 0.8 Da for fragment ions, thresholds: 0.1 for Δ Cn score and 2.0, 2.7, and 3.7 for minimum cross-correlation (Xcorr) values of +1, +2, and +3 charged ions, respectively).

3. Results and discussion

3.1. Characterization of PS-co-MAn

PS-*co*-MAn was synthesized by the RAFT method with a droplet micro-reactor. When using the droplet micro-reactor, molecular weight was well controlled with the variation of flow rates and polymerization time was greatly shortened [36]. Figure S2 (Supporting Information) shows detailed information for the droplet micro-reactor system and synthesis of the copolymer. Three kinds of PS-*co*-MAn were synthesized by varying the oil feed rate while the flow rate of organic solution was fixed at 2.0 μL min^{-1}. Copolymer molecular weight values determined by GPC are listed in Table S1 of Supporting Information. The results show that as oil feed rate increased, rate polymerization reaction time decreased with copolymer molecular weights ranging from 5.5 K to 12.3 K. The measured PDI values of all copolymers from GPC data were 1.1–1.2, indicating that they are highly uniform in polydispersity. According to the lowest PDI value among the three run conditions in Table S1, the flow rate ratio of 2:7 (organic solution:oil) was selected as suitable for further fabrication of ordered porous membranes using the breath figure method.

3.2. Evaluation of porous polymer membranes

To avoid the fragility of polymer membranes, copper mesh was prepared according to the reference [37]. The detailed process is shown in Supporting Information. SEM examination shows that the copper mesh surface was successfully eroded, as shown in Figure S3 (Supporting Information). Fig. 1 represents the preparation of porous polymer membranes on copper mesh. PS-*co*-MAn solution was delivered to the eroded copper mesh for membrane formation (Fig. 1), and SEM was used to examine the resulting polymer membranes coated on copper mesh. The SEM results in Fig. 3 show that triple layers of polymer coating on copper mesh (triple layers of membrane with one single copper mesh, Fig. 3E and F) provide a relatively uniform distribution of pores that is suitable for enzyme immobilization. The reproducibility of the porous polymer membrane preparation has been investigated by SEM (Figure S4) and the results displayed that the morphology of the porous polymer membrane was comparable and similar for fabricated at three runs. It should be noted that the thickness of the membrane was about 5 μm and a copper mesh about 50 μm, thus the thickness of one piece of copper mesh with three layers of copolymer membranes was about 65 μm.

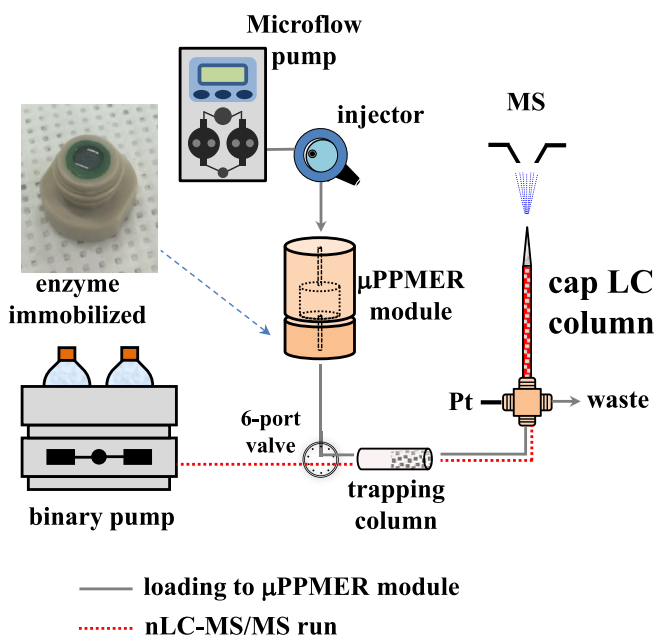**Fig. 2.** Configuration of on-line μPPMER-nLC-ESI-MS/MS system.

The pore size distribution curve displayed in Figure S5 shows that polymer membrane pore diameters range from 3.8 to 5.5 μm, and membrane porosity was 83.8%. Notably, pores in the polymer membranes provide micrometer scale domains to accommodate enzymes for proteolysis. The porous polymer membrane based on PS-co-MAn readily reacts with the amino group of enzyme molecules via ring-opening reactions, forming imides [38], as shown in Figure S6 (Supporting Information). Experimental results showed that the binding capacity of prepared porous polymer membranes was 0.8 ± 0.05 mg mL^{-1} (Supporting Information). This is much higher than the binding capacity of conventional porous membranes (0.1 mg/mL) [28], indicating that prepared membrane in this study is suitable for enzymatic reaction.

The morphology (Fig. 4A) of porous polymer membrane after enzyme immobilization and a schematic diagram (Fig. 4B) are displayed. Compared to the non-immobilized porous membrane (Fig. 3E and F), porous polymer membrane surface modified with trypsin displayed micropores and a rough surface with nanoparticles which were presumably crystalized salts from buffer solution (Fig. 4A). The immobilizing process and optimized immobilization conditions indicate that porous polymer membranes with copper mesh as a support matrix are favorable for immobilizing enzymes on membrane surfaces.

3.3. Activity evaluation of immobilized trypsin

The activity of immobilized trypsin was determined by the percentage of substrate hydrolyzed during passage through the membrane using BAEE as target molecules for digestion. The percentage of substrate hydrolyzed during passage through the membrane, H (%), can be obtained by the following equation,

$$H(\%) = \frac{A_0 - A_{BAEE}}{A_0} \times 100 \tag{1}$$

where A_0 and A_{BAEE} are peak areas of BAEE before and after enzyme digestion, respectively.

The Michaelis constant (K_m) and maximum velocity (V_{max}) of the Michaelis–Menten equation in equation (2) were used to determine the hydrolysis efficiency of immobilized trypsin and free trypsin in solution as
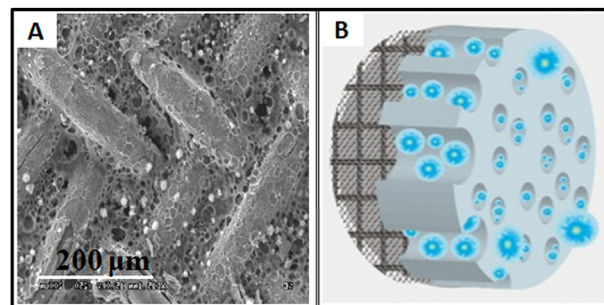

Fig. 4. SEM image (A) and schematic diagram (B) of trypsin immobilized on porous polymer membrane.

$$V = V_{max}[S]/(K_m + [S]) \tag{2}$$

where V and V_{max} are initial and maximum velocities, respectively, and [S] is target analyte concentration. Initial velocity represents the reaction rate measured immediately after a relatively short time period, while target analyte concentration remains approximately constant. Figure S7 in Supporting Information supports that hydrolysis efficiency is maximized at a flow rate of 0.03 mL min^{-1} (~70% BAEE were hydrolyzed) within the range of 0.01–1.0 mL min^{-1}. The effect of different layers of porous polymer membranes on digestion efficiency was investigated by stacking more layers to assure enzyme immobilization (the fabrication process of different layers of porous polymer membranes was described in the Supporting Information). As shown in Figure S8, the percentage of substrate hydrolyzed during passage through the membrane increased with triple polymer layers. From this, PPMER with triple layers of porous polymer membranes was selected for further study.

The kinetic study of PPMER was carried out at the above selected run conditions. From the Lineweaver–Burk plots for BAEE hydrolysis using PPMER shown in Figure S9, K_m and V_{max} values from non-linear regression were calculated as 2.3 mM and 3.12 mM min^{-1} (mg of typsin)$^{-1}$, respectively, while those from trypsin in free solution were 2.7 mM and 0.13 mM min^{-1} (mg of typsin)$^{-1}$. The measured K_m value of PPMER (2.3 mM) is somewhat
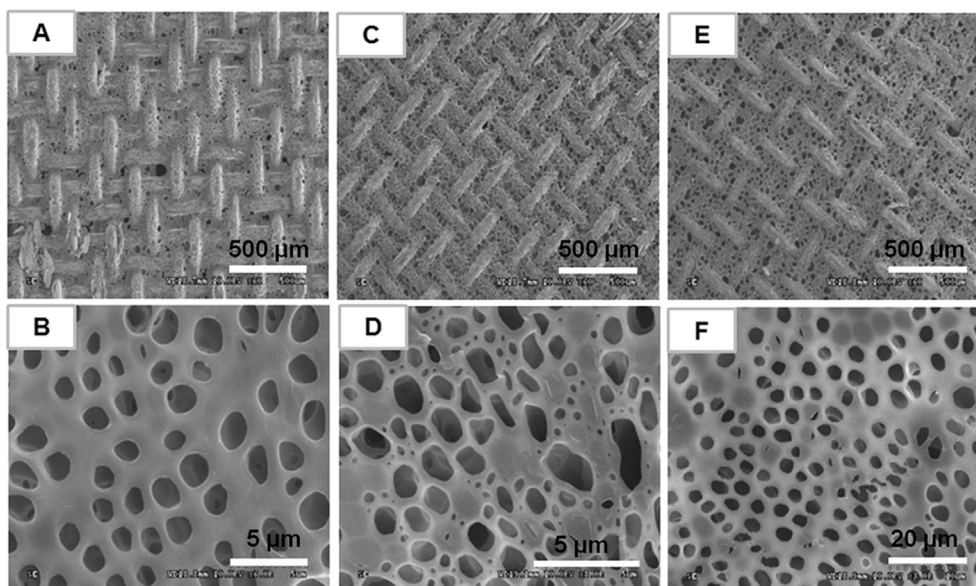

Fig. 3. SEM images of ordered porous polymer membranes. (A, B) Single layer; (C, D) Double layers; (E, F) Triple layers.

lower than that of free trypsin (2.7 mM), indicating that the structure and affinity of immobilized enzymes was not significantly altered from those in free solution. The V_{max} value of PPMER was about 24 times higher than that of free trypsin, demonstrating that a much higher reaction rate for PPMER was obtained at the same amount of trypsin. A relatively large amount of trypsin was immobilized in the limited microporous space, demonstrating that the enzymatic reactor was suitable for protein digestion.

The durability of PPMER was examined by repeating BAEE hydrolysis. The results displayed in Figure S10A show that enzyme activity can be maintained above 96% after nine runs compared to the first run. The percentage of substrate hydrolyzed during passage through the membrane, which was monitored for three weeks, showed less than 5.0% relative standard deviation in observed hydrolysis rates. However, it dropped below 60% after four weeks (Figure S10B).

3.4. Proteolysis efficiency in µPPMER-nLC-ESI-MS/MS

The immobilization of the trypsin onto the porous polymer membrane and the system of µPPMER-nLC-ESI-MS/MS were shown in Figure S1 and Fig. 2. The detail introduction was supplemented in experimental section.

The performance of on-line proteolysis was evaluated with two protein standards (BSA and cytochrome C) using µPPMER coupled with nLC-ESI-MS/MS as shown in Fig. 2 for on-line proteolysis and proteomic analysis. The efficiency of proteolysis was evaluated by varying the duration of tryptic digestion and the loading amount of standard proteins. Fig. 5 shows the comparison of base peak chromatograms (BPC's) for BSA peptides obtained by on-line µPPMER-nLC-ESI-MS/MS at (A) 10 min, (B) 30 min of periods for on-line digestion process together with (C) full MS spectra obtained at tr = 42.5−43.5 min, and data dependent collision induced dissociation (CID) spectra of peptide ions identified as (D) LGEYGFQNALIVR (m/z 740.4 at t_r = 43.3 min) and (E) ETYGD-MADCCEK (m/z of 710.9 at t_r = 42.6 min). The time duration

includes from the sample loading, on-line digestion, and injection to nLC. Each injection consisted of 500 ng BSA added to µPPMER at 5 µL/min. Apparently 10 min of duration time appears as insufficient for on-line digestion. As the duration time increased to 30 min, a significant number of peaks were observed with a successful identification of peptides as shown with an example of CID spectra in Fig. 5E.

The effect of time duration on tryptic digestion was exampled by comparing the sequence coverage of standard proteins and the number of peptides identified with varying periods (10 min, 20 min and 30 min) of flow pumping to µPPMER through the injector. Data regarding sequence coverage and number of identified peptides were based on triplicate measurements (n = 3) and are shown in Table 1. Each injection consisted of 500 ng BSA added to µPPMER at 5 µL/min. With 10 min of duration time, peptide sequence coverage was very low (~10%). Since the inner volume of µPPMER was ~29 µL, at least 6 min (at 5 µL/min) of pumping time was necessary for proteins to reach the µPPMER membrane surface. By considering that a certain period of time was required for sample to be transferred from autosampler to µPPMER, and to the trapping column, 10 min was not sufficient for the entire process. As duration time increased to 20 and 30 min, the sequence coverage from identified BSA peptides increased to 69% and 89%, respectively. The number of identified peptides increased to 53 and 79, respectively. Further increases in digestion time did not result in additional improvements in digestion. Therefore, 30 min of duration was selected for other evaluations. The total duration time (30 min in this work) includes sample loading to µPPMER, on-line proteolysis, and delivery of peptides to a trapping column of nLC-ESI-MS/MS. Since the digestion period in an on-line system can be estimated as ~80 s from the calculation of a residence time [28] based on the dimension of membrane, a majority of processing time came from delivery periods. Compared to a typical nLC-ESI-MS/MS run which requires 10 min of sample loading from autosampler to an analytical column for sample delivery and desalting, it needs to be improved by reducing the delivery period to µPPMER module. The
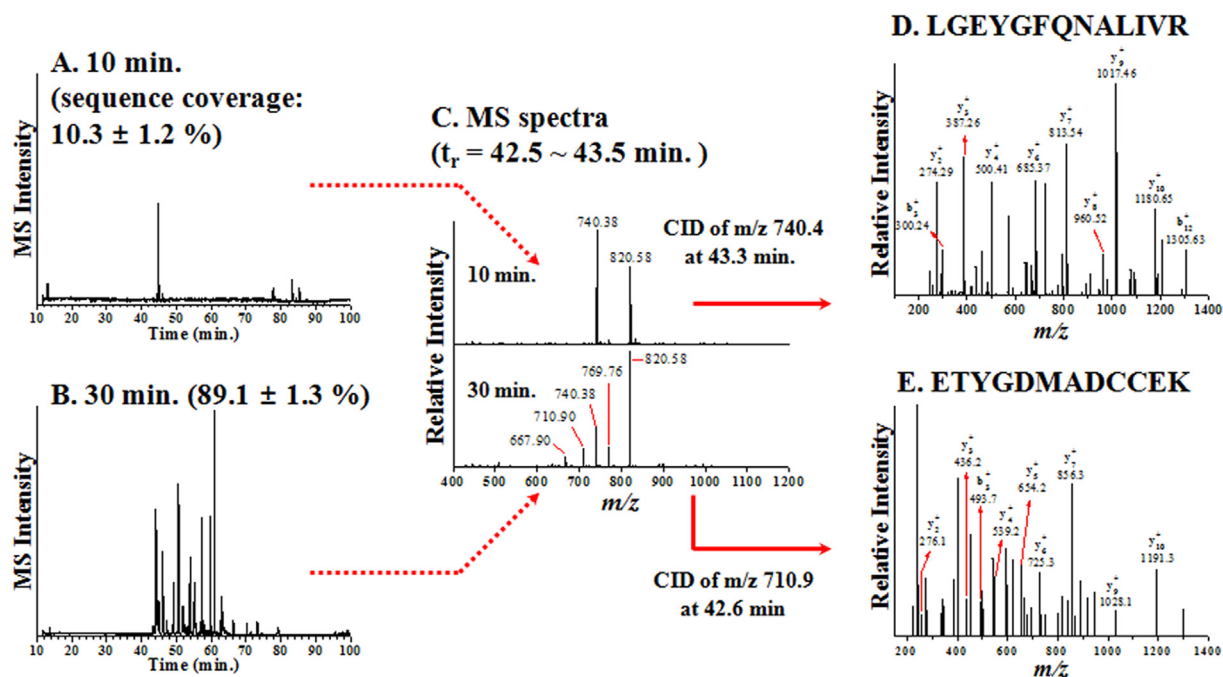
Fig. 5. Base peak chromatograms of tryptic peptides of bovine serum albumin (BSA) obtained by on-line µPPMER-nLC-ESI-MS/MS analysis at (A) 10 min and (B) 30 min of periods for on-line digestion process including sample loading. (C) Full MS spectra at t_r = 42.5−43.5 min and data dependent CID spectra of a peptide ion identified as (D) GEYGFQNALIVR for precursor ion m/z of 740.4 at t_r = 43.3 min and (E) ETYGDMADCCEK for precursor ion m/z of 710.9 at t_r = 42.6 min.

Table 1
Efficiency of time duration for tryptic digestion of 500 ng of BSA (n = 3) using online μPPMER-nLC-ESI-MS/MS method.

Time of digestion (min)	Sequence coverage (%)	Number of peptides
10	10.3 ± 1.2	4 ± 1
20	69.3 ± 3.8	53 ± 3
30	89.1 ± 1.3	79 ± 2

duration time can be further reduced when pore size of μPPMER membrane can be reduced, which enables one to use a faster sample delivery to μPPMER. Use of a μPPMER module of a smaller inner volume may also reduce the sample loading period. Reducing the dead volume can increase collision rate of proteins with enzyme, eventually enhance mass transfer rate between proteins and enzymes. However in this study, it was focused on evaluating the enzymatic digestion efficiency of μPPMER membrane.

The digestion limit was examined by decreasing protein standard loading amount (cytochrome C and BSA) from 1 μg to 10 ng. The amino acid sequences of BSA identified from on-line μPPMER-nLC-ESI-MS/MS were listed in Table S2 compared among different duration time of digestion process: gray for identified sequences at 10 min, yellow for peptides additionally identified at 20 min and green at 30 min. When 1 μg of protein was loaded, BSA resulted in 92% sequence coverage while cytochrome C yielded 64% sequence coverage. When loading amount was decreased to 200 ng, the observed sequence coverage values were 81.9% and 53.0% for BSA and cytochrome C, respectively. The number of identified peptides did not significantly decrease until 200 ng of injection. The sequence coverage data for cytochrome C were lower than those of BSA peptides because cytochrome C has a smaller number of tryptic peptides (105 amino acids) than BSA (607 amino acids). While large proteins may have a longer period of retention within pores during their cleavage process than small ones, smaller proteins may retain shortly within pores and exit the reactor without a complete digestion. Since μPPMER in the present experiment had relatively large pore sizes, it presumably resulted in incomplete proteolysis of smaller proteins and loss of protein fragments through the enzyme reactor during flow penetration. This was confirmed by comparing the numbers of BSA peptides with mis-cleavage between in-solution digestion and on-line digestion. Table 2 compares the sequence coverage of BSA peptides between in-solution digestion followed by nLC-ESI-MS/MS and on-line μPPMER-nLC-ESI-MS/MS

by varying injection amounts. It clearly shows that sequence coverage of identified peptides by on-line digestion certainly increased about 25% from in-solution digestion. The numbers of identified peptides with on-line digestion showed distinct increases in three injection amounts. Especially, on-line digestion showed a better efficiency at a lower injection amount of proteins. However, numbers of mis-cleaved peptides were certainly lower (25 vs 48 in 1000 ng injection) with in-solution digestion than with on-line digestion. This supports that the μPPMER had relatively large pores through which peptides with incomplete digestion were swept out. Elution of mis-cleaved peptides can be found in Figure S11 which shows more crowded peaks with both urine and plasma samples using μPPMER. Nonetheless, this study shows a potential that on-line digestion using μPPMER can be utilized for the efficient digestion of small amount of proteins. Especially, on-line digestion of 200 ng of BSA (3 pmol) using μPPMER yielded ~80% of sequence coverage (Table 3), demonstrating that μPPMER-nLC-ESI-MS/MS could be an alternative on-line characterization method for proteomic analysis.

3.5. Application of μPPMER-nLC-ESI-MS/MS to human urinary and plasma proteome samples

Developed μPPMER was applied to characterize human urinary and plasma proteome samples. Figure S11 shows the comparison of BPC's obtained from urine and plasma samples between in-solution digestion and on-line digestion using μPPMER. The numbers of proteins from both samples in Figure S11 were based on a 10 μg injection of proteins for on-line μPPMER-nLC-ESI-MS/MS and on digested peptides (equivalent to 10 μg proteins) for in-solution digestion and nLC-ESI-MS/MS. Proteins identified from both plasma and urine sample are listed in Table S3. Figure S12 compares the numbers of proteins identified with on-line μPPMER-nLC-ESI-MS/MS to those identified by in-solution digestion and nLC-ESI-MS/MS. The in-solution digestion method yielded with 235 proteins from 503 unique peptides for urine samples and 414 proteins from 807 unique peptides for plasma samples. In comparison, 274 proteins (from 781 unique peptides) and 476 proteins (from 1184 unique peptides) were identified by on-line digestion using μPPMER. In addition, 182 urinary and 340 plasma proteins were commonly found with both digestion methods. While 53 urinary proteins and 74 plasma proteins were only found with the in-

Table 2
Sequence coverage (%) and the number of identified peptides along with mis-cleavage from BSA obtained between in-solution digestion and on-line μPPMER-nLC-ESI-MS/MS methods at different amounts of BSA (10 ng, 100 ng and 1000 ng).

Amount of injected protein (ng)	Sequence coverage (%)		Number of identified peptides		Number of mis-cleaved peptides	
	In-solution digestion	μPPMER	In-solution digestion	μPPMER	In-solution digestion	μPPMER
1000	73.2	92.7 ± 1.4	51	83 ± 2	25	48 ± 3
100	49.1	63.6 ± 2.3	21	42 ± 3	16	25 ± 2
10	0.0	9.2 ± 1.5	0	3 ± 1	0	2 ± 1

Table 3
Comparison of sequence coverage (%) and number of identified peptides obtained by on-line μPPMER-nLC-ESI-MS/MS with cytochrome C and BSA (enzymatic reaction time was fixed at 30 min, n = 3).

Amount of injected protein (ng)	Sequence coverage (%)		Number of identified peptides	
	BSA	Cytochrome C	BSA	Cytochrome C
1000	92.7 ± 1.4	64.5 ± 3.9	83 ± 2	26 ± 2
500	89.1 ± 1.3	58.1 ± 2.5	79 ± 2	22 ± 3
200	81.9 ± 6.7	53.0 ± 0.5	63 ± 3	17 ± 3
100	63.6 ± 2.3	17.5 ± 3.4	42 ± 3	4 ± 2
10	9.2 ± 1.5	3.8 ± 6.6	3 ± 1	1 ± 1

solution method, the on-line digestion method yielded additional identification of 92 urinary proteins and 136 plasma proteins. Overall, data indicates that the on-line digestion method yielded more than 10% of proteins (~50% increase in total peptides) compared to the in-solution method.

According to the subcellular locations (based on UniProtKB) of proteins exclusively found by both methods, the number and percentage of membrane proteins found by only the on-line method increased to 31.5% (29 proteins) from 18.9% (10) with the in-solution method for urinary proteins and increased to 23.6% (32) from 13.5% (10) for plasma proteins. The percentages of cytoplasmic (27.9 vs. 27.2% for on-line vs. in-solution method) and nucleus proteins (17.6 vs. 13.0%) did not change significantly. This indicates that on-line digestion of μPPMER provides an increased chance of protein-enzyme reaction due to the local increase in enzyme concentration within microporous membrane structures. In addition, μPPMER enhances accommodation of hydrophobic proteins within membrane pores, allowing proteolysis to occur.

4. Conclusions

This work features a novel type of PPMER created with the breath figure method using PS-*co*-MAn as a porous polymer membrane with copper mesh as support. The enzymatic reaction rate of immobilized trypsin was about 24 times higher than that of unbound enzymes in solution. Using BSA and Cyt-C as model substrates, the enzyme reactor μPPMER displayed its capability for on-line proteolysis prior to bottom-up proteomic analysis using nLC-ESI-MS/MS. Meanwhile, the proposed μPPMER showed equivalent or higher efficiency in enzymatic reactions with human urinary and plasma proteome samples compared to the in-solution method. This result is due to local confinement of proteolysis within porous domains to yield higher efficiency in identifying membrane proteins. While present study demonstrates that μPPMER provides a new method for protease immobilization, works are needed to improve the efficiency by reducing pore size of μPPMER membrane and duration time for sample loading from autosampler through μPPMER to nLC system. In conclusion, the developed μPPMER-nLC-ESI-MS/MS system can be expanded to create a comprehensive protein analysis protocol for deglycosylation of N-linked glycoproteins/glycopeptides using lectin-specific binding affinity either by immobilizing enzymes or lectins in the reactor.

Appendix A. Supplementary data

Supplementary data related to this article can be found at http://dx.doi.org/10.1016/j.aca.2015.11.042.

References

[1] M.L. Ye, Y.B. Pan, K. Cheng, H.F. Zou, Protein digestion priority is independent of protein abundances, Nat. Methods 11 (2014) 220–222.
[2] C.Y. Shi, C.H. Deng, Y. Li, X.M. Zhang, P.Y. Yang, Hydrophilic polydopamine-coated magnetic graphene nanocomposites for highly efficient tryptic immobilization, Proteomics 14 (2014) 1457–1463.
[3] J. Yang, L. Qi, H.M. Ma, Y. Chen, Fabrication of nylon membrane-based microfluidic chips and its application in color sensing of glucose, Chem. J. Chin. Univ. 11 (2012) 2405–2410.
[4] A.J. Percy, D.C. Schriemer, Rheostatic control of tryptic digestion in a micro-scale fluidic system, Anal. Chim. Acta 657 (2010) 53–59.
[5] Y. Liu, H.X. Wang, Q.P. Liu, H.Y. Qu, B.H. Liu, P.Y. Yang, Improvement of proteolytic efficiency towards low-level proteins by an antifouling surface of alumina gel in a microchannel, Lab Chip 10 (2010) 2887–2893.
[6] J.W. Cooper, J. Chen, Y. Li, C.S. Lee, Membrane-based nanoscale proteolytic reactor enabling protein digestion, peptide separation, and protein identification using mass spectrometry, Anal. Chem. 75 (2003) 1067–1074.
[7] S. Andreasen, B. Fejerskov, A.N. Zelikin, Biocatalytic polymer thin films: optimization of the multilayered architecture towards in situ synthesis of anti-proliferative drugs, Nanoscale 6 (2014) 4131–4140.
[8] Y. Shen, W. Guo, L. Qi, J. Qiao, F.Y. Wang, L.Q. Mao, Immobilization of trypsin via reactive polymer grafting from magnetic nanoparticles for microwave-assisted digestion, J. Mater. Chem. B 1 (2013) 2260–2267.
[9] S. Lin, D. Yun, D.W. Qi, C.H. Deng, Y. Li, X.M. Zhang, Novel microwave-assisted digestion by trypsin-immobilized magnetic nanoparticles for proteomic analysis, J. Proteome Res. 7 (2008) 1297–1307.
[10] C. Fan, Z.M. Shi, Y.T. Pan, Z.F. Song, W.J. Zhang, X.Y. Zhao, F. Tian, B. Peng, W.J. Qin, Y. Cai, X.H. Qian, Dual matrix-based immobilized trypsin for complementary proteolytic digestion and fast proteomics analysis with higher protein sequence coverage, Anal. Chem. 86 (2014) 1452–1458.
[11] W.J. Qin, Z.F. Song, C. Fan, W.J. Zhang, Y. Cai, Y.J. Zhang, X.H. Qian, Trypsin immobilization on hairy polymer chains hybrid magnetic nanoparticles for ultra fast, highly efficient proteome digestion, facile ^{18}O labeling and absolute protein quantification, Anal. Chem. 84 (2012) 3138–3144.
[12] J. Sheng, L. Zhang, J.P. Lei, H.X. Ju, Fabrication of tunable microreactor with enzyme modified magnetic nanoparticles for microfluidic electrochemical detection of glucose, Anal. Chim. Acta 709 (2012) 41–46.
[13] Y.Q. Yin, Y. Xiao, G. Lin, Q. Xiao, Z. Lin, Z.W. Cai, An enzyme–inorganic hybrid nanoflower based immobilized enzyme reactor with enhanced enzymatic activity, J. Mater. Chem. B 3 (2015) 2295–2300.
[14] S.K. Kailasa, H.-F. Wu, Recent developments in nanoparticle-based MALDI mass spectrometric analysis of phosphoproteomes, Microchim. Acta 181 (2014) 853–864.
[15] S.K. Kailasa, H.-F. Wu, Nanomaterial-based miniaturized extraction and pre-concentration techniques coupled to matrix-assisted laser desorption/ionization mass spectrometry for assaying biomolecules, Trends Anal. Chem. 65 (2015) 54–72.
[16] T. Tsukatania, K. Matsumoto, Fluorometric quantification of total d-gluconate by a flow-injection system using an immobilized-enzyme reactor, Anal. Chim. Acta 530 (2005) 221–225.
[17] C. Dartiguenave, H. Hamad, K.C. Waldron, Immobilization of trypsin onto 1,4-diisothiocyanatobenzene-activated porous glass for microreactor-based peptide mapping by capillary electrophoresis: effect of calcium ions on the immobilization procedure, Anal. Chim. Acta 663 (2010) 198–205.
[18] T.R. Besanger, R.J. Hodgson, J.R.A. Green, J.D. Brennan, Immobilized enzyme reactor chromatography: optimization of protein retention and enzyme activity in monolithic silica stationary phases, Anal. Chim. Acta 564 (2006) 106–115.
[19] D.S. Peterson, T. Rohr, F. Svec, J.M.J. Fréchet, Enzymatic microreactor-on-a-chip: protein mapping using trypsin immobilized on porous polymer monoliths Molded in channels of microfluidic devices, Anal. Chem. 74 (2002) 4081–4088.
[20] J.Y. Kim, S.Y. Lee, S.K. Kim, S.R. Park, D. Kang, M.H. Moon, Development of an online microbore hollow fiber enzyme reactor coupled with nanoflow liquid chromatography-tandem mass spectrometry for global proteomics, Anal. Chem. 85 (2013) 5506–5513.
[21] J.Y. Kim, D. Oh, S.K. Kim, D. Kang, M.H. Moon, Isotope-coded carbamidomethylation for quantification of N-glycoproteins with online microbore hollow fiber enzyme reactor-nanoflow liquid chromatography-tandem mass spectrometry, Anal. Chem. 86 (2014) 7650–7657.
[22] Y.H. Lin, J.S. Ren, X.G. Qu, Catalytically active nanomaterials: a promising candidate for artificial enzymes, Acc. Chem. Res. 47 (2014) 1097–1105.
[23] L. Qiao, Y. Liu, S.P. Hudson, P.Y. Yang, E. Magner, B.H. Liu, A nanoporous reactor for efficient proteolysis, Chem. Eur. J. 14 (2008) 151–157.
[24] K. Qian, J.J. Wan, X.D. Huang, P.Y. Yang, B.H. Liu, C.Z. Yu, A smart glycol-directed nanodevice from rationally designed macroporous materials, Chem. Eur. J. 16 (2010) 822–828.
[25] S.J. Li, C. Wang, Z.Q. Wu, J.J. Xu, X.H. Xia, H.Y. Chen, Real-time monitoring of mass-transport-related enzymatic reaction kinetics in a nanochannel-array reactor, Chem. Eur. J. 16 (2010) 10186–10194.
[26] S.S. Cao, L. Fang, Z.Y. Zhao, Y. Ge, S. Piletsky, A.P.F. Turner, Hierachically structured hollow silica spheres for high efficiency immobilization of enzymes, Adv. Funct. Mater. 23 (2013) 2162–2167.
[27] Z.J. Chen, Z.H. Guan, M.R. Li, Q.H. Yang, C. Li, Enhancement of the performance of a platinum nanocatalyst confined within carbon nanotubes for asymmetric hydrogenation, Angew. Chem. Int. Ed. 50 (2011) 4913–4917.
[28] F. Xu, W.H. Wang, Y.J. Tan, M.L. Bruening, Facile trypsin immobilization in polymeric membranes for rapid, efficient protein digestion, Anal. Chem. 82 (2010) 10045–10051.
[29] Y.J. Tan, D.X. Sui, W.H. Wang, M.H. Kuo, G.E. Reid, M.L. Bruening, Phosphopeptide enrichment with TiO₂ modified membranes and investigation of Tau protein phosphorylation, Anal. Chem. 85 (2013) 5699–5706.

[30] Y.J. Tan, W.H. Wang, Y. Zheng, J.L. Dong, G. Stefano, F. Brandizzi, R.M. Garavito, G.E. Reid, M.L. Bruening, Limited proteolysis via millisecond digestions in protease-modified membranes, Anal. Chem. 84 (2012) 8357–8363.

[31] M. Hartmann, X. Kostrov, Immobilization of enzymes on porous silicas-benefits and challenges, Chem. Soc. Rev. 42 (2013) 6277–6289.

[32] H. Bai, C. Du, A.J. Zhang, L. Li, Breath figure arrays: unconventional fabrications, functionalizations, and applications, Angew. Chem. Int. Ed. 52 (2013) 12240–12255.

[33] L.S. Wan, J.W. Li, B.B. Ke, Z.K. Xu, Ordered microporous membranes templated by breath figures for size-selective separation, J. Am. Chem. Soc. 134 (2012) 95–98.

[34] J.T. Lai, D. Filla, R. Shea, Functional polymers from novel carboxyl-terminated trithiocarbonates as highly efficient RAFT agents, Macromolecules 35 (2002) 6754–6756.

[35] J.F. Ma, Z. Liang, X.Q. Qiao, Q.L. Deng, D.Y. Tao, L.H. Zhang, Y.K. Zhang, Organic-inorganic hybrid silica monolith based immobilized trypsin reactor with high enzymatic activity, Anal. Chem. 80 (2008) 2949–2956.

[36] P.H. Hoang, C.T. Nguyen, J. Perumal, D.P. Kim, Droplet synthesis of well-defined block copolymers using solvent-resistant microfluidic device, Lab Chip 11 (2011) 329–335.

[37] Y.Z. Feng, I.S. Cho, P.M. Rao, L.L. Cai, X.L. Zheng, Sol-flame synthesis: a general strategy to decorate nanowires with metal oxide/noble metal nanoparticles, Nano Lett. 13 (2013) 855–860.

[38] T. Bayer, K.J. Eichhorn, K. Grundke, H.J. Jacobasch, Macromol. Chem. Phys. 200 (1999) 852–857.